THE JOURNAL OF BIOLOGICAL CHEMISTRY VOL. 283, NO. 39, pp. 26748–26758, September 26, 2008

β-Barrel Proteins That Reside in the *Escherichia coli* Outer Membrane *in Vivo* Demonstrate Varied Folding Behavior *in Vitro*[*] [S]

Received for publication, April 9, 2008, and in revised form, July 18, 2008 Published, JBC Papers in Press, July 19, 2008, DOI 10.1074/jbc.M802754200

Nancy K. Burgess, Thuy P. Dao, Ann Marie Stanley, and Karen G. Fleming[1]

From the T. C. Jenkins Department of Biophysics, Johns Hopkins University, Baltimore, Maryland 21218

Little is known about the dynamic process of membrane protein folding, and few models exist to explore it. In this study we doubled the number of *Escherichia coli* outer membrane proteins (OMPs) for which folding into lipid bilayers has been systematically investigated. We cloned, expressed, and folded nine OMPs: outer membrane protein X (OmpX), OmpW, OmpA, the *crcA* gene product (PagP), OmpT, outer membrane phospholipase A (OmpLa), the *fadl* gene product (FadL), the *yaet* gene product (Omp85), and OmpF. These proteins fold into the same bilayer *in vivo* and share a transmembrane β-barrel motif but vary in sequence and barrel size. We quantified the ability of these OMPs to fold into a matrix of bilayer environments. Several trends emerged from these experiments: higher pH values, thinner bilayers, and increased bilayer curvature promote folding of all OMPs. Increasing the incubation temperature promoted folding of several OMPs but inhibited folding of others. We discovered that OMPs do not have the same ability to fold into any single bilayer environment. This suggests that although environmental factors influence folding, OMPs also have intrinsic qualities that profoundly modulate their folding. To rationalize the differences in folding efficiency, we performed kinetic and thermal denaturation experiments, the results of which demonstrated that OMPs employ different strategies to achieve the observed folding efficiency.

The number of high resolution membrane protein structures increases each year (1). These structures provide a static picture of the membrane protein native state but reveal nothing about the dynamic folding process that formed them. Despite these advances in structural biology, the question remains: how does a polypeptide chain encode a structure that folds into a biological membrane?

Proteins adopt a variety of folds, yet those that span a biological membrane exhibit only one of two general architectures, either the α-helix or the β-barrel. These transmembrane (TM)[2] motifs satisfy the hydrogen bonding requirements of the peptide backbone in the hydrophobic environment of the cellular membrane (2, 3). Interestingly, these motifs are found in different membranes *in vivo*. Most bilayers contain proteins with an α-helix TM motif, but β-barrel proteins only reside in the outer membranes of chloroplasts (4), mitochondria (5, 6), and Gram-negative bacteria (7). To traverse a membrane, proteins adopt one of only two folds, yet their ability to insert and assume their native structures remains a complex issue that is not well understood.

In vivo, α-helical and β-barrel membrane proteins insert into their respective biological membranes via different molecular machinery. The protein factors that aid bilayer insertion of an α-helix motif have been identified, and an elegant system using *in vivo* machinery has been developed to study α-helix insertion into membranes (8, 9). For β-barrel proteins, also called outer membrane proteins (OMPs), a few of the *in vivo* folding factors that facilitate insertion have been proposed only recently and are not yet fully understood (10). Although the *in vivo* OMP folding pathway must yet be completely defined, it has been shown that several OMPs can fold spontaneously into synthetic membranes (11–15). The ability of OMPs to spontaneously insert into synthetic vesicles has two important implications. First, there is no additional energy input required for the folding reaction to occur. Therefore, the native state of the protein is an equilibrium structure and thermodynamic measurements of stability can be made *in vitro* that have relevance in the biological setting. Second, a system composed of synthetic vesicles has significantly fewer variables than the heterogeneous milieu of biological membranes. Furthermore, synthetic vesicles can be modified systematically to dissect the molecular details of how bilayer properties influence OMP folding. Thus, in the absence of a clearly defined *in vivo* folding pathway, *in vitro* folding studies can identify both the protein and the bilayer characteristics that promote folding and insertion of membrane proteins.

Unlike water, the relatively homogeneous solvent for soluble proteins, the biological membrane can vary in its lipid composition, overall charge, and gross morphology. The most valuable *in vitro* membrane protein folding system would therefore mimic the *in vivo* lipid conditions that a protein encounters.

* This work was supported by Grant MCB0423807 from the National Science Foundation. The costs of publication of this article were defrayed in part by the payment of page charges. This article must therefore be hereby marked "*advertisement*" in accordance with 18 U.S.C. Section 1734 solely to indicate this fact.

[S] The on-line version of this article (available at http://www.jbc.org) contains supplemental Fig. S1 and table S1.

[1] To whom correspondence should be addressed: 3400 N. Charles St., Baltimore, MD 21218. Tel.: 410-516-7256; Fax: 410-516-5451; E-mail: karen.fleming@jhu.edu.

[2] The abbreviations used are: TM, transmembrane; OMP, outer membrane protein; PG, phosphatidylglycerol; PE, phosphatidylethanolamine; PC, phosphatidylcholine; LUV, large unilamellar vesicle; SUV, small unilamellar vesicle; diC, diacylglycerol.

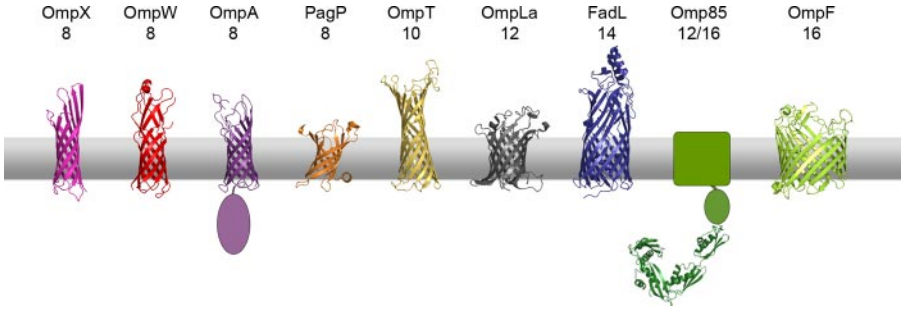

FIGURE 1. **Structures of OMPs used in this study.** Structures for each OMP are shown in their relative orientation in the outer membrane (*gray bar*). Across the top of the figure are listed the *names* and *numbers* of β-strands that constitute the transmembrane barrel of each protein. Omp85 is postulated to have either 12 strands (46) or 16 strands (44), so both numbers are shown. Images were made in PyMOL with the following files from the Protein Data Bank: 1QJ8 (OmpX), 2F1V (OmpW), 1BXW (OmpA), 1THQ (PagP), 1I78 (OmpT), 1QD5 (OmpLa), 1T16 (FadL), 2QDF (Omp85 POTRA domains), and 2OMF (OmpF). Protein domains of unknown structure are represented as geometric shapes: a *purple oval* for the periplasmic region of OmpA, a *green oval* for one of the five periplasmic domains of Omp85, and a *green square* for the transmembrane domain of Omp85. Furthermore, OmpF most often occurs as a trimer, but only a single monomer is shown.

Proteins in the outer membrane of *Escherichia coli* reside in an asymmetric bilayer in which the outer leaflet is made of the glycolipid lipopolysaccharide and the inner leaflet is composed of phospholipids with either the phosphatidylglycerol (PG) or phosphatidylethanolamine (PE) head group (16, 17). This asymmetry can be recreated *in vitro* with planar bilayers, but such bilayers do not remain stable on the time scale of OMP folding experiments (18) and therefore are not amenable to folding studies. Instead, vesicles composed entirely of phospholipids have been used to study OMP folding (11–15). Despite the asymmetry of outer membranes, it is likely that phospholipids are the most appropriate model for folding studies, because OMPs first encounter the inner leaflet (composed entirely of phospholipids) as they fold into the outer membrane *in vivo* (10).

The most extensively studied β-barrel folding model in phospholipid vesicles is outer membrane protein A (OmpA). Studies of OmpA have revealed how insertion occurs (19–23) and have measured the stability of the native structure in different lipid environments (24–27). The principles garnered from these studies allow conclusions to be drawn for how OmpA behaves, but they cannot reliably be applied to all OMPs until the behaviors of other proteins are observed in the same environment. Moreover, folding studies have been performed on other OMPs (12–15), but no comprehensive folding screen exists that facilitates comparison between proteins. To directly compare the folding propensities of membrane proteins, we probed the folding conditions of nine different β-barrel OMPs: OmpX, OmpW, OmpA, the *crcA* gene product (PagP), OmpT, outer membrane phospholipase A (OmpLa), the *fadl* gene product (FadL), the *yaet* gene product (Omp85), and OmpF.

The OMPs we chose all reside in the outer membrane of *E. coli*. Despite inhabiting the same bilayer environment *in vivo* and sharing a common TM motif, the primary sequences of these nine OMPs could not be aligned altogether or in pairwise BLAST queries (data not shown). Furthermore, the structure of each OMP varies from the next (Fig. 1). These model OMPs have barrel sizes ranging from eight β-strands (OmpX, OmpW, OmpA, and PagP) to 16 β-strands (OmpF). Their extramembrane structures also vary. OmpA and Omp85 have periplasmic domains as large as their TM domains, whereas FadL and OmpT have significant amounts of structure extending from their barrels toward the extracellular side of the biological membrane.

The study of these nine OMPs constitutes the largest set of OMPs evaluated in tandem to date. In this work, we have established OmpW, OmpT, OmpLa, FadL, and Omp85 as novel models for folding studies. For purposes of direct comparison, we included OMPs that have previously been shown to fold into phospholipid bilayers *in vitro*: OmpA (11), OmpF (12), OmpX (28), and PagP (15). Our data set doubles the number of *E. coli* OMPs for which folding has been systematically examined in lipid bilayers. Further, because these OMPs are sequentially and structurally diverse yet fold into the same environment *in vivo*, our results allowed the deduction of broad rules that define folding similarities and differences.

EXPERIMENTAL PROCEDURES

Vesicle Preparation—Lipids dissolved in chloroform (Avanti Polar Lipids) were dried to a thin film in glass vials under a gentle stream of nitrogen gas. Lipid films were evacuated for at least 3 h to remove residual solvent and stored at −20 °C until use. Lipid films were reconstituted in buffer containing 2 mM EDTA (Fluka) and 10 mM borate (Sigma), pH 10. Vesicles used in pH studies were brought up in the same concentration of appropriate buffers at various pH values. To make small unilamellar vesicles (SUVs), lipids reconstituted in buffer were sonicated on ice for 50 min with a 50% duty cycle with a Branson Sonifier as described previously (25). Large unilamellar vesicles (LUVs) were made by extruding reconstituted lipids 11 times through a 0.1 μM filter using a mini-extruder (Avanti Polar Lipids).

Cloning and Expression of OMPs—Primers were designed to encompass the mature forms of the OMPs and add NdeI (5′) and BamHI (3′) sites. Primers are listed in supplemental Table S1. OMP genes were amplified using ExTaq polymerase (Takara) from an overnight growth of *E. coli* K12 MG1655 (29). The PCR products were cut with restriction enzymes and ligated into a pET11a vector. The resulting plasmids were transformed into a laboratory supply of electrocompetent DH5α cells. The sequences were confirmed by double-stranded DNA sequencing using the T7 promoter and T7 terminator primers for all clones. Additional primers were designed and used for Omp85 to cover the length of the insert. The expression products were confirmed by matrix-assisted laser desorption ionization (MALDI) mass spectrometry at the Johns Hopkins Medical Institute.

Plasmids were transformed into BL21(DE3) Star™ cells (Invitrogen). Transformed cells were grown in 500 ml of LB medium to an optical density of 0.6 at 600 nm before expression was induced by the addition of 1 mM β-D-1-thiogalactopyranoside. Cells continued to incubate for 3–4 h at 37 °C and were

harvested by centrifugation (5500 rpm, 30 min, 4 °C). Pellets were resuspended in 25 ml of lysis buffer (50 mM Tris, pH 8, 40 mM EDTA, 125 μl of 20 mg ml^{-1} lysozyme) and incubated for 30 min on ice before being sonicated three times for 1 min at a 50% duty cycle. Brij-35 (Sigma) was added to a final concentration of 0.1%. Inclusion bodies were centrifuged (6000 rpm, 30 min, 4 °C) and washed twice by resuspension in 25 ml of wash buffer (10 mM Tris, pH 8, 2 mM EDTA) followed by centrifugation (6000 rpm, 30 min, 4 °C). Cells were resuspended a third time in wash buffer and aliquoted into 3-ml fractions before a final centrifugation (6000 rpm, 30 min, 4 °C). Supernatant was discarded, and inclusion body pellets were stored at −20 °C.

OMP Folding—Inclusion body pellets were dissolved in 8 M urea (ultra pure grade, Amresco), 2 mM EDTA, and 10 mM borate, pH 10, to a final concentration of 100 μM protein. Protein concentration was determined by measuring the absorbance at 280 nm. The extinction coefficients for each OMP were determined using Sequence Analysis software (Informagen), with the exception of OmpLa, for which we used a previously published value (90,444 M^{-1} cm^{-1}) (30).

OMPs were refolded by rapid dilution into 3.2 mM synthetic lipid or 2.3 mg ml^{-1} lipid extract in folding buffer (1 M urea, 2 mM EDTA, 10 mM borate, pH 10) to a final concentration of 4 μM protein. Folding temperatures were controlled by incubating reactions in a PTC-200 Peltier thermal cycler (MJ Research). Overnight reactions were incubated for 15 h.

SDS-PAGE—Folding reactions were quenched by adding 5× SDS gel-loading buffer (31) to a final dilution of 1× SDS gel-loading buffer. Samples were stored at −20 °C, if not immediately loaded onto a gel. 15 μl of sample (or only 5 μl of Omp85 sample because of its high molecular weight) were then loaded on a precast gel (Bio-Rad) without boiling. OmpX, OmpW, and PagP required gels with 4–20% acrylamide continuous gradient to resolve the folded and unfolded populations, but all other OMPs could be resolved on 10% acrylamide gels. After electrophoresis, gels were stained with Coomassie Blue and scanned digitally. Densitometry was performed using ImageJ software.[3] The linear regions of the densitometry were determined by measuring the density of standards of known protein amounts. The fraction folded is calculated by dividing the intensity of the folded band by the sum of the intensities of both the folded and unfolded bands.

Folding Efficiency—We defined folding efficiency as the fraction of folded protein quantified at the overnight (15 h) time point.

Folding Kinetics—After folding was initiated, small aliquots of the folding reaction were removed and quenched with 5× SDS-PAGE loading buffer at the following time points: 5, 10, 20, 30, 45, 60, 120, 180, 300, 420, 720, 1200, and 1800 s. The fraction folded for each time point was determined by SDS-PAGE and densitometry as described above. We fit the results of folding kinetics to either a single exponential equation,

$$y = y_0 + A\exp(-kt) \quad \text{(Eq. 1)}$$

or a double exponential equation,

$$y = y_0 + A_1\exp(-k_1t) + A_2\exp(-k_2t) \quad \text{(Eq. 2)}$$

where y is the fraction folded at a given time, t, y_0 is the fraction folded as time approaches infinity, k_1 and k_2 are rate constants, and A_1 and A_2 are the negative amplitudes associated with each rate constant. The burst phase is calculated as a sum of y_0, A_1, and A_2. The lag phase is defined as the first time point at which fraction folded was equal to or greater than 0.05. The reported values and error bars equal the average and standard deviations, respectively, of three independent kinetic experiments.

RESULTS

Thinner Bilayers and Smaller Vesicles Promote Folding Efficiency—To probe the bilayer properties that affect OMP folding, we incubated OMPs overnight with synthetic vesicles composed of a variety of lipids. The overnight time point (15 h) was chosen because it is an experimentally convenient time point for screening a large number of conditions and is intermediate to the incubation times used in previous folding studies (12, 14, 21). Although some of the folding reactions were not complete by 15 h, this time point was sensitive to the fastest and most efficient folding events.

The buffer we used contained 10 mM borate, pH 10, 2 mM EDTA, and 1 M urea. Previous OMP studies have used residual amounts of urea under folding conditions (11–14, 21), yet OmpA can fold in 4 M urea (25) and PagP can fold in 7 M urea (15). Although OMPs can fold into synthetic vesicles at a variety of urea concentrations, we chose a low concentration of urea (1 M) in which to conduct this folding screen.

To determine the fraction of protein that folded under a given condition, we used SDS-PAGE. Even before the first OMP structure was solved, it was observed by SDS-PAGE that OMPs share a characteristic called "heat modifiability"; that is, adding SDS to OMPs captures the folded and unfolded populations present in solution. During electrophoresis, these populations migrate to different positions (32, 33). When OMPs are solubilized in SDS and subsequently boiled, they lose their native β-content and migrate to their expected molecular weight on polyacrylamide gels (33). However, unboiled samples of folded OMPs retain a high content of β-structure (33) as well as their activity (12, 15, 30, 34) and migrate to a different position than the unfolded form. Because SDS-PAGE can distinguish between folded and unfolded populations, it has become a standard assay for assessing OMP folding. Fig. 2 shows that the OMPs we cloned and expressed all demonstrate this heat modifiability, as expected for each protein (12, 15, 21, 30, 34–40).

To determine the folding propensities under the most native-like conditions, we tested whether OMPs could fold into extracts prepared from their native lipids. We purchased two *E. coli* lipid extracts from Avanti Polar Lipids: total extract (57.5% PE, 15.1% PG, 9.8% cardiolipin, and 17.6% of uncharacterized mass) and polar extract (67.0% PE, 23.2% PG, 9.8% cardiolipin). These *E. coli* extracts could not be extruded to make LUVs; therefore we made SUVs by sonication. We incubated OMPs with SUVs of native lipids for 15 h, quenched folding by adding SDS-loading buffer, and performed electrophoresis on the unboiled samples. The fraction folded for each protein was

[3] Program authored by Wayne Rasband.

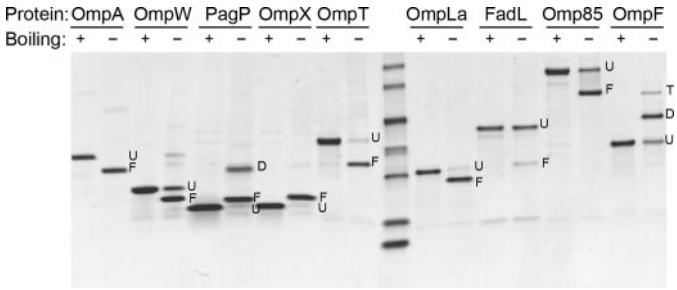

FIGURE 2. **OMPs demonstrate heat modifiability.** OMPs were folded into $diC_{10}PC$ LUVs at a lipid to protein ratio of 800:1 in a buffer containing 1 M urea, 2 mM EDTA, and 10 mM borate, pH 10. The folding reactions were incubated at 37 °C for 15 h before being quenched by adding 5× SDS-PAGE loading buffer to a final concentration of 1×. Samples were then split in two, and one was boiled at 95 °C for 5 min. Boiled and unboiled samples were loaded onto a 4–20% continuous gradient acrylamide gel for electrophoresis. The folded (*F*) and unfolded (*U*) populations of each protein are designated at the *right* of each band. For a few OMPs, folded dimers (*D*) and trimers (*T*) are also indicated. Because there were not enough lanes available on a single gel, this image is the composite of two different gels that have been lined up in the middle of the figure by a lane of protein standards. From *top* to *bottom*, the standard bands represent molecular masses of 100, 75, 50, 35, 25, 15, and 10 kDa.

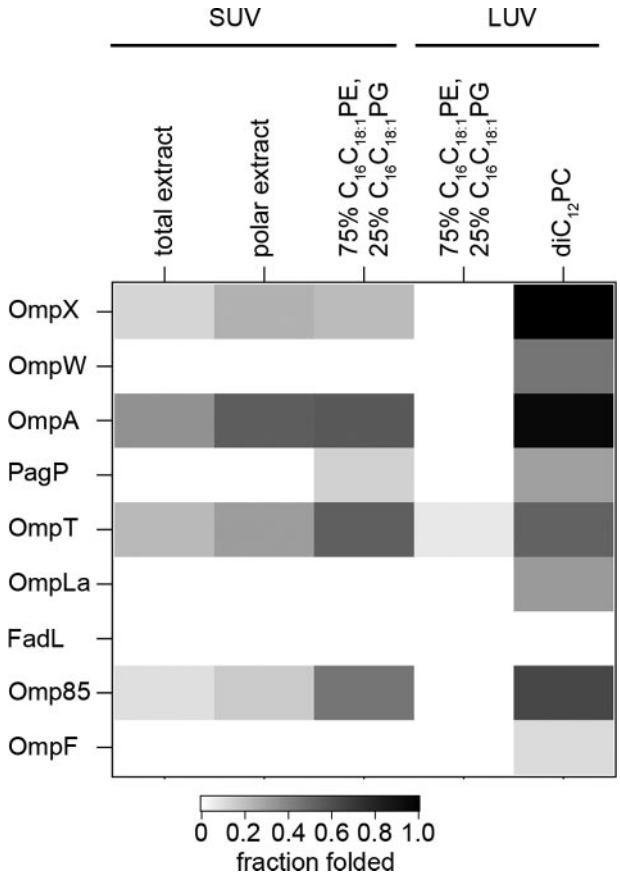

FIGURE 3. ***In vivo*-like bilayers did not support folding for all OMPs.** We tested OMP folding in bilayers of both natural lipids (polar or total *E. coli* extracts) and synthetic lipids (25% $C_{16}C_{18:1}$PG/75% $C_{16}C_{18:1}$PE or 100% diC_{12}PC). Each reaction was incubated at 37 °C for 15 h in buffer containing 1 M urea, 2 mM EDTA, and 10 mM borate, pH 10. Folding reactions were quenched by adding 5× SDS-PAGE loading buffer to a final concentration of 1×. Samples were loaded onto acrylamide gels without boiling. After electrophoresis, the relative folded and unfolded populations were determined by densitometry. The fraction folded values were converted to grayscale based on the key at the bottom of the graph. The lipids and vesicles used in each reaction are designated at the *top* of each column, and the *name* of each OMP is listed at the *left*.

determined by densitometry of the scanned gels. Fig. 3 shows that total and polar extracts gave similar results. In both extracts, a small population of only four of the nine proteins (OmpX, OmpA, OmpT, and Omp85) could fold into SUVs of native lipids.

We then tested the ability of synthetic lipids to recapitulate the native lipids result. Fig. 3 shows that SUVs composed of synthetic lipids with a composition similar to the native extracts (75% $C_{16}C_{18:1}$PE, 25% $C_{16}C_{18:1}$PG) gave comparable results. We therefore conclude that pure preparations of synthetic lipids can reproduce the results obtained using native lipids. Further, unlike the native lipid extracts, the synthetic lipids could be extruded through 100-nm filters to make LUVs, which allowed us to assess the effect of bilayer curvature on OMP folding. With the exception of OmpT, we found that none of the OMPs folded into LUVs of synthetic lipids of native-like composition.

Because less than half of the OMPs could fold into extracted lipids or native-like synthetic lipids, we tried bilayers with phosphatidylcholine (PC) head groups. Although *E. coli* do not contain any PC in their bilayers, PC-containing membranes are used in many aspects of OMP research, including computational simulations (41), ion channel measurements (42, 43), and folding studies (11–14, 22). Moreover, the TM β-barrels found in eukaryotes are located in the outer membranes of mitochondria, which are composed primarily of PC lipids, further supporting the notion that membranes composed of synthetic PC lipids are appropriate *in vitro* substitutes for biological lipid bilayers. Consistent with this idea, the data shown in Figs. 3 and 4 demonstrate that PC lipids promote *in vitro* folding of all the OMPs in this study.

Using PC lipids, we further investigated how acyl chain length, acyl chain saturation, and vesicle size influenced folding. The results of folding OMPs into PC lipids are shown in Fig. 4, where the lipids are listed from left to right in order of increasing number of methylene groups and the OMPs are listed on the left side by increasing number of β-strands, starting from OMPs with eight β-strands (OmpX, OmpW, OmpA, and PagP) to 16 β-strands (OmpF). In both LUVs (Fig. 4*A*) and SUVs (Fig. 4*B*), nearly all OMPs fold most efficiently in bilayers composed of shorter-chain lipids, and thus demonstrate a folding dependence on bilayer thickness. Two of the smallest barrels, OmpX and OmpA, fold very efficiently under almost all conditions. Omp85 has the highest molecular weight and is predicted to be a barrel of either 12 or 16 strands (44–46), but it also folds to a high yield under most lipid conditions. This finding suggests that the folding dependence on bilayer thickness is likely not determined by barrel size. To confirm that vesicles were indeed present in the shortest acyl chain length ($diC_{10}PC$), we visualized them using electron microscopy (supplemental Fig. S1).

In addition to the dependence on acyl chain length, another trend emerged from the data in Fig. 4. A comparison of the results from folding OMPs into LUVs (Fig. 4*A*) and SUVs (Fig. 4*B*) revealed that OMPs generally have higher folding efficiencies when incubated with SUVs. This result is consistent with

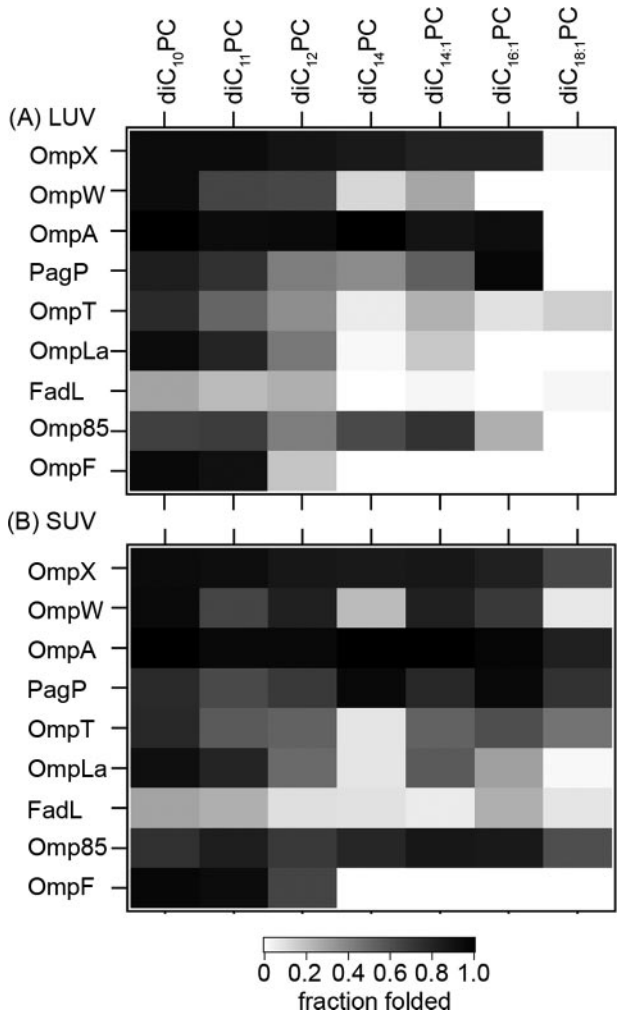

FIGURE 4. **Fraction folded of OMPs in various PC lipids.** OMPs were incubated overnight (15 h) at 38.3 °C in various lipids at a lipid to protein ratio of 800:1. The buffer was 1 M urea, 2 mM EDTA, and 10 mM borate, pH 10. Folding reactions were quenched by adding 5× SDS-PAGE loading buffer to a final concentration of 1×. Samples were loaded onto acrylamide gels without boiling. After electrophoresis, the relative folded and unfolded populations were determined by densitometry. The fraction folded values were converted to grayscale based on the *key* at the *bottom* of the figure. The lipids used in each reaction are designated at the *top* of each column, and the *name* of each OMP is listed at the *left*. OMPs were folded into LUVs (*A*) and SUVs (*B*).

the folding trends we observed for the native-like synthetic lipids in Fig. 3.

The Effect of Incubation Temperature Varies for Each OMP—Increasing the temperature raises the thermal energy available for reactions, and it has been suggested that a higher folding temperature improves folding efficiencies of OMPs (14, 20). We tested the effect of incubation temperature by repeating the folding experiments at temperatures ranging from 30 to 50 °C. Fig. 5 shows the trends observed for folding OMPs into LUVs at various temperatures, and the data obtained in SUVs were similar (data not shown). Overall, the effect of temperature on folding efficiency is varied. The folding efficiency of each OMP increased, decreased, or exhibited no change with respect to temperature. The incubation temperature seemed most influential on the higher molecular weight OMPs (OmpF and Omp85). These OMPs displayed reduced folding efficiencies at higher temperatures and neither of them could fold into most lipid bilayers at 50 °C. However, the effect of temperature on folding did not necessarily correlate with barrel size. Consider the eight-stranded barrels: increasing the incubation temperature from 30 to 50 °C decreases the folding efficiency of OmpX and OmpA, increases the folding efficiency of PagP, and has almost no effect on the folding efficiency of OmpW. Therefore, the incubation temperature modulates the folding of each OMP differently, an effect that is not fundamentally related to the number of strands in the barrel.

OMPs Fold Most Efficiently under Basic pH Conditions—In bacteria, OMPs fold while in the periplasm, where the pH is determined by the extracellular environment and can vary (47). Previous *in vitro* studies of OMPs have also used a range of pH values. Although PagP folding was observed at pH 8 (15), OmpF folding was optimal at pH 6.5 (12), and OmpA folded most efficiently (12) but demonstrated the least stability (26) at pH 10. The general effect of pH on OMP folding efficiency is unknown in the absence of a direct comparison in identical lipid environments. We therefore investigated the influence of pH using $diC_{12}PC$ LUVs because it afforded maximum sensitivity to both increases and decreases in folding efficiency in our initial screen at pH 10 (Fig. 4). Fig. 6 shows the results of folding OMPs at a range of pH values and demonstrates that all OMPs folded to higher efficiencies at higher pH values. Under these conditions, OmpF folds optimally at pH 8, whereas the other OMPs fold most efficiently at pH 9 or 10. In the pH range used here, the bilayer remains neutral (48). These OMPs all have a theoretical pI between 5 and 6 (calculated using SEDNTERP (49)) and thus have a net negative charge in basic conditions. This charge appears to improve OMP folding efficiency.

Lipids with PE or PG Head Groups Have Varied Effects on OMP Folding—To further probe how lipids with PE and PG head groups influenced the folding efficiencies of OMPs, we used a host-guest system to introduce these lipids in the background of membranes composed of PC-containing lipids. We prepared vesicles with either 5% (mol/mol) or 20% (mol/mol) of either $diC_{12}PG$ or $diC_{12}PE$ in host bilayers of $diC_{12}PC$ and determined the folding efficiency. As a control, we visualized the vesicles by electron microscopy to confirm that bilayers were formed under these conditions (supplemental Fig. S1).

The *first column* in Fig. 7, *A* and *B*, shows the fraction folded for each OMP in bilayers of $diC_{12}PC$, which can be compared with the subsequent *columns* that display folding efficiency in bilayers where the guest lipid has been introduced. When lipids with PG and PE head groups are present, the folding efficiency diminishes for OmpLa, FadL, and OmpF. Proteins that exhibit high folding efficiency in the $diC_{12}PC$ bilayer (OmpX, OmpA, Omp85) are unaffected by the presence of the guest lipids. In contrast, both $diC_{12}PE$ and $diC_{12}PG$ enhanced the folding of OmpT and PagP. With the exception of PagP, these results generally recapitulated our initial findings for the natively extracted lipids; the OMPs in which folding efficiency was unaffected by or enhanced by PE or PG lipids are those for which we observed folding into SUVs of the natively extracted lipids.

Cholesterol Diminishes Folding Efficiency—Cholesterol is found natively in eukaryotic membranes. Although the bacterial proteins studied here do not encounter cholesterol *in vivo*, cholesterol is known to modulate of membrane fluidity.

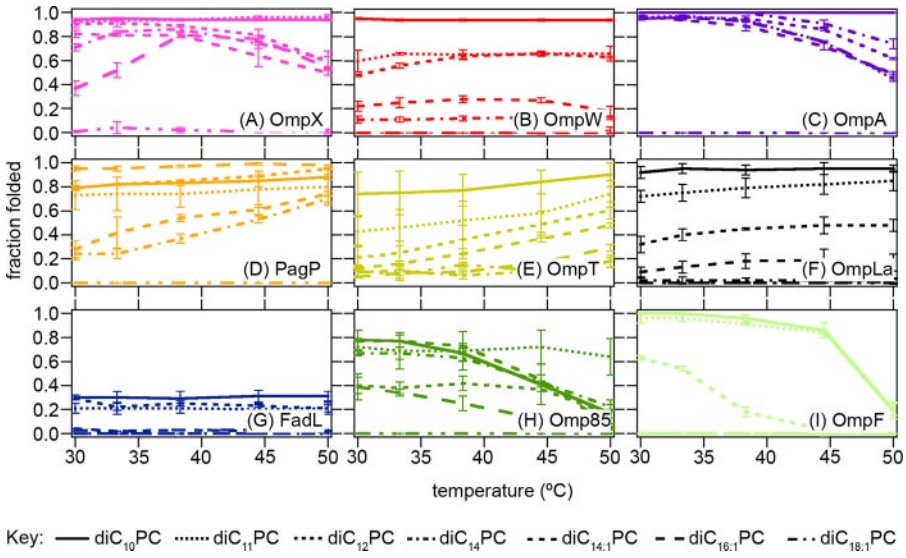

FIGURE 5. **Fraction folded of OMPs at various temperatures.** OMPs were folded into LUVs for 15 h at incubation temperatures ranging from 30 to 50 °C, and the fraction folded was determined by densitometry of SDS-PAGE results. In each *panel*, the *vertical axis* defines the fraction folded, and the *horizontal axis* shows the incubation temperature of the folding reaction in °C. The *lines* in each *panel* connect the observed fraction folded at a discrete temperature. Each line represents a different lipid as indicated at the bottom of the figure. Markers were left off of the graphs for clarity. The *error bars* associated with each data point are displayed and represent the standard deviation of three independent trials. Each panel represents a different protein: *A*, OmpX; *B*, OmpW; *C*, OmpA; *D*, PagP; *E*, OmpT; *F*, OmpLa; *G*, FadL; *H*, Omp85; *I*, OmpF.

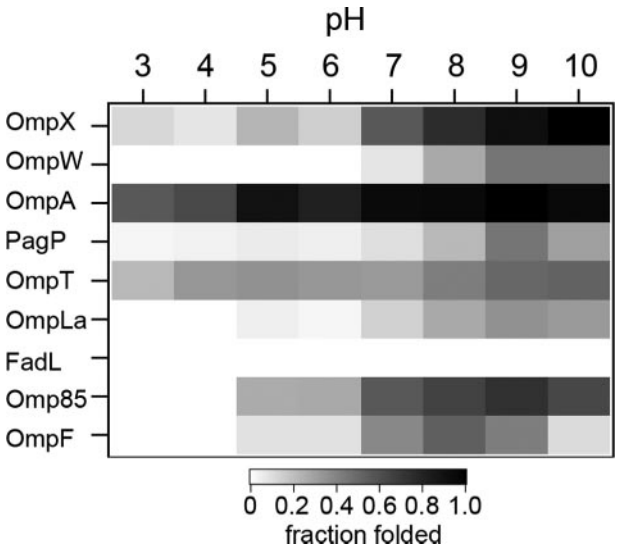

FIGURE 6. **Fraction folded of OMPs at various pH values.** OMPs were incubated for 15 h in $diC_{12}PC$ LUVs at a lipid to protein ratio of 800:1. The buffer was 1 M urea, 2 mM EDTA, and 10 mM buffer at various pH values. Folding reactions were quenched by adding 5× SDS-PAGE loading buffer to a final concentration of 1×. Samples were loaded onto acrylamide gels without boiling. After electrophoresis, the relative folded and unfolded populations were determined by densitometry. The fraction folded values were converted to grayscale based on the *key* at the *bottom* of the figure. The pH of each reaction is listed at the *top* of the figure, and the *name* of each OMP is listed at the *left*.

Furthermore, some cholesterol-containing membranes of eukaryotes accommodate β-barrel proteins (5, 6). Therefore, observing how the presence of cholesterol affects β-barrel protein folding would be informative as to how membrane fluidity, as well as native eukaryotic conditions, influences the folding process. In eukaryotes, cholesterol is found in different quantities in different membranes (50), so we chose to introduce a low (5%) and a high (20%) concentration of cholesterol into $diC_{12}PC$ LUVs. Fig. 7*C* demonstrates that increased cholesterol in this host-guest system decreased folding efficiency of all bacterial OMPs. *In vivo*, β-barrels are found in mitochondrial membranes (5, 6), where cholesterol concentration is low (50), but not in plasma membranes, where the cholesterol concentration is high (50). The conditions that promote folding in Fig. 7*C* are consistent with the lipid compositions where β-barrels are found *in vivo*.

How Are Folding Efficiencies Influenced by Kinetic or Thermodynamic Behavior?—All experiments described thus far reveal an important facet of OMP folding: no single lipid condition universally supports folding for all the OMPs to the same efficiency. This discovery is striking because these OMPs have evolved to fold into the same conditions *in vivo*, and one might further intuit that OMP folding generally would be optimized to fold into the same lipid bilayers. In contrast, our data suggest that OMPs fold optimally in different environments, and thus characteristics inherent to each protein must also profoundly influence folding.

The physical basis underlying the folding efficiencies we measured at the 15-h time point cannot be known from this screen. Proteins that fold to a higher efficiency than others in the same environment at a given time point may fold faster, intrinsically have more stability, or reflect variations in both folding rates and stability. Similarly, proteins that fail to demonstrate folding at 15 h may fold extremely slowly or may not be stable in the given lipid environment. The finding that OMPs that inhabit the same bilayer *in vivo* demonstrate vastly different folding profiles *in vitro* can be rationalized by determining the stability and kinetic behavior of each OMP.

OMPs Fold More Slowly into Thicker Bilayers—The details of the kinetic behavior have been studied thoroughly only for OmpA (14, 19–23), and limited kinetic data are available on only three other OMPs: OmpF (12), PagP (15), and the major outer membrane protein of *Fusobacterium nucleatum* (FomA) (14). Among these previous studies, there is no consensus on conditions. The experimental parameters vary in protein to lipid ratio, buffer, pH, length of observation time, temperature, lipid type, and vesicle size. Changing just one parameter such as temperature (14, 19, 22, 23), lipid type (14, 20), vesicle size (21), or protein to lipid ratio (20)[4] can have drastic effects on the kinetic behavior. Because kinetic behavior can reveal the mechanistic details of folding, the effect of all of these parameters should be tested. Although a full analysis is beyond the scope of

[4] N. K. Burgess and K. G. Fleming, unpublished results with OmpLa.

the current study, we can address the origins of the chain length dependence on folding efficiency.

We monitored the kinetics of each OMP folding reaction into LUVs of three different lipids, $diC_{10}PC$, $diC_{11}PC$, and $diC_{12}PC$, for 1800 s (30 min). These experiments were performed in triplicate; representative data sets are shown in Fig. 8. The results demonstrate that all OMPs folded faster into the thinner $diC_{10}PC$ bilayers. Although this has been shown to be true for OmpA (20) and FomA (14), we have demonstrated here that the kinetics of all OMPs are similarly slowed by thicker bilayers.

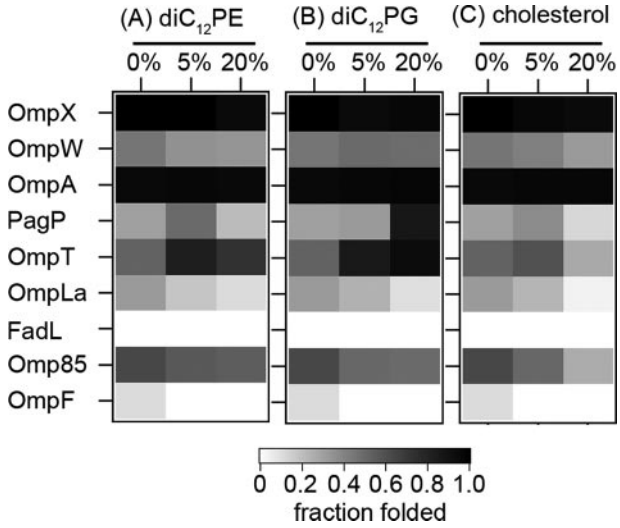

FIGURE 7. **Influence of PE and PG head groups and cholesterol on fraction folded of OMPs.** We used $diC_{12}PC$ LUVs as a host bilayer for introducing guest molecules. OMPs were incubated with bilayers composed of $diC_{12}PC$ and 5 or 20% of (*A*) $diC_{12}PE$, (*B*) $diC_{12}PG$, or (*C*) cholesterol. The percent and kind of guest molecule is indicated at the *top* of the figure, and the proteins are listed at the *left*. Reactions took place at 37 °C for 15 h with an 800:1 lipid to protein ratio. Folding was quenched by the addition of SDS-PAGE loading buffer. The fraction folded was assessed by densitometry of PAGE results and then converted to grayscale based on the *key* at the *bottom* of the figure.

To determine the details of the kinetic behavior under these conditions, we tried fitting each data set to either a single- or double-exponential rate equation. The data sets that could be sufficiently explained by either a single or double exponential equation are shown by *fit lines* in Fig. 8. These fits provide values for the observed rate constants, the relative amount of species that is associated with each rate constant, and the folding efficiency as time approaches infinity. These values are summarized graphically in Fig. 9. For some reactions, the entire amplitude could not be accounted for by the fitted rates because a portion of the folding reaction had finished before it could be detected by SDS-PAGE (in less than 5 s). We call the folding that occurred during mixing the burst phase. The largest burst phase was demonstrated by OmpX in $diC_{10}PC$. About 80% of OmpX folds in less than 5 s, making the folding rate of OmpX in $diC_{10}PC$ too fast to be measured by SDS-PAGE. Although OmpX is the most extreme case, most OMPs demonstrated a burst phase in $diC_{10}PC$ (Fig. 9*A*).

Apart from revealing a burst phase, most OMP kinetics can be fitted to a double-exponential equation containing a fast rate, on the order of $10-80 \times 10^{-3}\ s^{-1}$, and a slow rate, on the order of $1-5 \times 10^{-3}\ s^{-1}$ (Fig. 9). Comparing the folding rates for each OMP between $diC_{10}PC$ and $diC_{11}PC$ bilayers, we see that the change in bilayer thickness slows the fast rates only slightly and has no substantial effect on the slow rates. Thus, it is not likely that a change in rate accounts for the slower kinetics observed in thicker bilayers. Rather, what changes most between the kinetic behavior of OMPs in $diC_{10}PC$ and $diC_{11}PC$ bilayers is the amplitude of each rate. In $diC_{10}PC$, most of the kinetic behavior for each OMP is driven by the burst and fast phases (Fig. 9*A*). In $diC_{11}PC$, there is no burst phase demonstrated by any OMP, and the relative amplitude of the fast phase is also reduced (Fig. 9*B*). The slower kinetics of folding observed in thicker bilayers is not due to slower rates but is a result of a higher portion of the population participating in slower rates. This effect is corroborated by results from FomA (14).

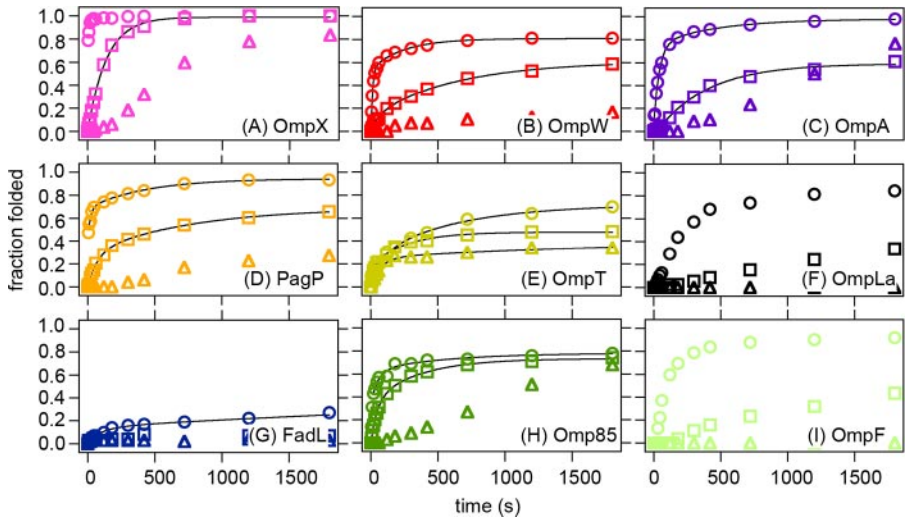

FIGURE 8. **Preliminary kinetic observations of OMP folding.** The folding of each OMP was observed at 37 °C over time in LUVs composed of $diC_{10}PC$ (○), $diC_{11}PC$ (□), and $diC_{12}PC$ (△). After folding reactions began, small aliquots were removed and quenched by SDS-PAGE loading buffer at different time points. The fraction folded (*vertical axis*) was obtained by densitometry of SDS-PAGE results. The *horizontal axis* shows elapsed time in seconds. Experiments were performed in triplicate, and each panel shows representative data from a single protein: *A*, OmpX; *B*, OmpW; *C*, OmpA; *D*, PagP; *E*, OmpT; *F*, OmpLa; *G*, FadL; *H*, Omp85; *I*, OmpF. The *black lines* were fitted to data sets that could be described by a single- or double-exponential rate equation. All other data sets demonstrated a lag or burst phase that could not be fitted by the same model.

Not every OMP was adequately fit by single- or double-exponential rate equations, yet the difficulties encountered while fitting these data are instructive. Many curves could not be fit because the initial folding did not begin until 60–300 s after the reaction began. We call this initial delay in folding the lag phase. This lag phase can be fit if the folding kinetic scheme is known for these conditions. Extensive work on OmpA has shown that OmpA folds by a sequential pathway with various intermediates (19–23). Some of the same data have been reinterpreted to suggest that the measured kinetic rates reflect parallel pathways (14). Applying either model to any of the proteins here with the

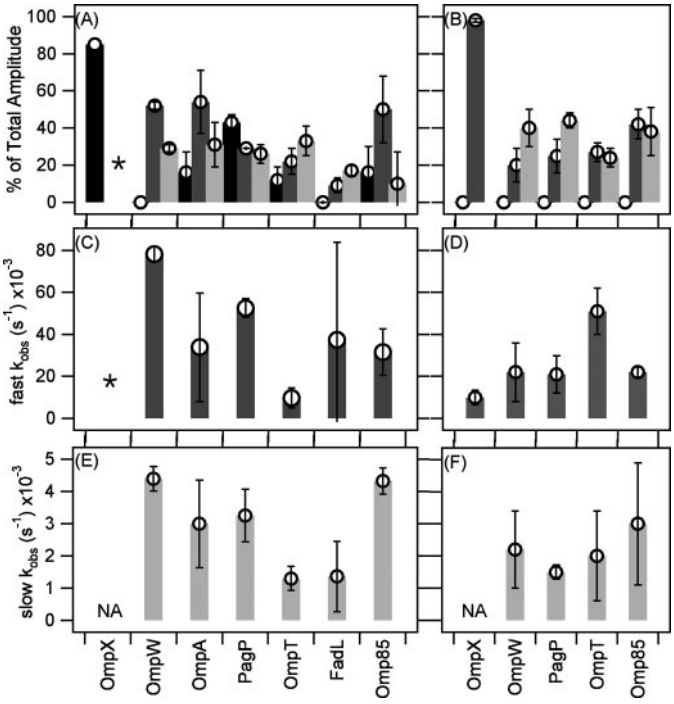

FIGURE 9. **Amplitudes and rates of kinetic fits.** The amplitudes and rate constants from the kinetic experiments that could be described by single- and double-exponential equations are listed here. The *values* and *errors* represent the average ± standard deviation, respectively, of the three independent trials. The *names* of the proteins are listed at the *bottom* of the figure. *A* and *B* show the amplitudes of the burst phase (*black bars*), fast phase (*dark gray bars*), and slow phase (*light gray bars*) of the kinetic fits. *C* and *D* show the fast rates of the kinetic fits. *E* and *F* show the slow rates of the kinetic fits. The *left panels* (*A*, *C*, and *E*) are from kinetic experiments in $diC_{10}PC$, and the *right panels* (*B*, *D*, and *F*) are from the kinetic experiments in $diC_{11}PC$. *NA* stands for not applicable and was placed on the graph for rates that do not exist. The *five-point asterisk* indicates rates that were too fast to be measured.

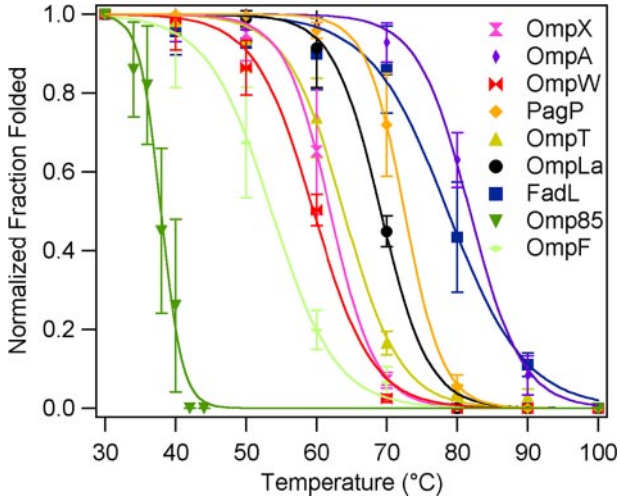

FIGURE 10. **Resistance to thermal denaturation.** OMPs were incubated at 37 °C with $diC_{10}PC$ LUVs at a lipid to protein ratio of 800:1. Folding reactions were quenched by addition of 5x SDS-PAGE loading buffer to a final concentration of 1x. Samples were then heated for 10 min at a range of temperatures (*horizontal* axis) before PAGE. The densitometry results were normalized to the amount of protein that remained folded after incubation at 30 °C and is indicated on the *vertical* axis. The data are fit to the equation of a sigmoid.

current data should be done with caution because there is not sufficient data to determine which folding scheme is valid. Furthermore, it has yet to be shown whether all OMPs share a universal folding pathway or whether each OMP folds by a unique scheme. More extensive kinetic analysis must be performed to dissect the kinetic scheme for each OMP and to understand exactly how the lag phase contributes to it.

Until the kinetics are more extensively interrogated and understood, we can make some empirical statements about the lag phase. We defined the lag phase as the first time point at which equal to or more than 0.05 fraction folded is observed. Based on this criterion, the lag phase is only present in OmpLa (20 s) and OmpF (30 s) in $diC_{10}PC$ LUVs. In $diC_{11}PC$ LUVs, the lag phases of OmpLa and OmpF are longer (both 300 s), and OmpA also demonstrates a lag phase (60 s). In $diC_{12}PC$ LUVs, only OmpT has no lag phase. All other OMPs demonstrate a lag phase of 60 to 420 s in $diC_{12}PC$ LUVs. Because both the length of the lag phase and the number of OMPs demonstrating lag phases increase in thicker bilayers, we concluded that this kinetic behavior depends on bilayer thickness and that thicker bilayers universally delay formation of tertiary structure.

OMPs Demonstrate Varied Resistance to Thermal Denaturation—Differences in folding efficiencies may also reflect variations in OMP thermodynamic stability, as protein stability is intimately linked to its solvent. The most effective way to compare stabilities between proteins is to measure them directly. However, the conditions under which OMP stability can be measured have been established for only a single protein, OmpA (25), and the experimental requirements to measure stability cannot be met under all lipid conditions (51). No unique set of conditions tested here promotes complete folding for every OMP at 15 h (Figs. 2–7). Without a single set of conditions that completely populates the folded state for every OMP, we can neither rigorously measure nor directly compare their stabilities. As a proxy for the means to determine stabilities for each OMP, we assessed the resistance to thermal denaturation, a parameter that is often related to stability.

We folded OMPs into $diC_{10}PC$ LUVs overnight and then quenched the folding reactions with SDS-loading buffer. With the OMPs now solvated by $diC_{10}PC$/SDS mixed micelles, prior to electrophoresis we heated each sample for 10 min at a range of temperatures. The resistance to thermal denaturation is inferred from the fraction folded that remained following the 10-min incubation. Fig. 10 shows that the resistance to thermal denaturation is varied. FadL is one of the OMPs most resistant to thermal denaturation, and yet it folds least efficiently under most conditions (Fig. 4). In contrast, Omp85 is the first to unfold when the temperature is increased but folds more efficiently than several of the proteins in this study (Fig. 4). In all cases, however, the resistance to thermal stability for each OMP was well described by a sigmoidal curve, and the data were fitted to obtain a temperature at which the folded population of each OMP remains 50% folded (T_{50}).

Recognizing that this T_{50} may have limited rigorous thermodynamic value, we addressed whether it might have practical use by comparing it with a variety of parameters that could be calculated for each protein. We found that there was no correlation between T_{50} and barrel size, molecular weight, pI, hydrophobic thickness of the structure (7), or the calculated free energy of transfer from water to the hydrophobic environment (7) (data not shown).

DISCUSSION

Novel OMP Folding Models Are Established—Previous to this study only six other β-barrel proteins had been shown to insert spontaneously into a phospholipid bilayer *in vitro*: OmpA (11), OmpF (12), PagP (15), OmpX (28), FomA (14), and the eukaryotic voltage-dependent anion-selective channel (13). Despite the existence of several folding models, the data they have provided are impossible to compare because of experimental variations including bilayer composition, temperature, and incubation time. Due to a sparse number of models and a lack of experimental uniformity, no definitive rules existed that were applicable to all OMPs. For the purpose of determining the general principles that govern OMP folding, we provided the first comprehensive study of a large set of OMPs folding into identical environments.

OMPs Follow Trends in Folding Efficiency—For most OMPs, thicker bilayers decrease folding efficiency (Fig. 4). This observation is consistent with previous FomA (14) and OmpA (20) studies that were conducted with a limited set of lipids. Here we show that the magnitude of the effect of thicker bilayers varies between OMPs. Although OmpX folding efficiency is slightly decreased between $diC_{10}PC$ bilayers and $diC_{16:1}PC$ bilayers, OmpF folding efficiency decreases precipitously from $diC_{10}PC$ bilayers to $diC_{12}PC$ bilayers (Fig. 4). The effect cannot be uniquely quantified for all OMPs, but thicker bilayers inhibit spontaneous insertion of each β-barrel protein to some degree. The kinetic experiments also corroborate this trend; Fig. 8 shows that OMPs fold more slowly into thicker bilayers.

The preference of OMPs for thinner bilayers may have biological importance. It has been suggested that OMPs selectively insert into the outer membrane rather than the inner membrane because the outer membrane is thinner (20). This proposal is supported by data from the structures of proteins localized to each membrane: the average hydrophobic thickness of bacterial OMPs (23.7 ± 1.3 Å) is shorter than that of bacterial inner membrane proteins (29.0 ± 2.6 Å) (52). This proposal is also supported by the data shown here. OMPs fold more efficiently into $diC_{10}PC$ bilayers, which are 26.5 Å thick (53), than into $diC_{12}PC$ bilayers, which are 30.5 Å thick (53). Several of the OMPs (FadL, OmpLa, OmpF) could not fold into $diC_{14}PC$ bilayers, which are 34 Å thick (53). These results may reflect how OMPs choose the proper membrane for insertion.

We also examined the effect of bilayer curvature on folding efficiency by using both SUVs and LUVs. We found that the folding efficiency of OMPs generally increased when incubated with bilayers of increased curvature (Figs. 3 and 4) but that the effect varies between OMPs. Surrey *et al.* observed this effect under a limited number of conditions: OmpA folds more efficiently into SUVs than LUVs (21), but OmpF folding into $diC_{14}PC$ at a single temperature (30 °C) is not affected by bilayer curvature (12).

The effect of incubation temperature on folding efficiency had been explored previously in a few cases. Higher temperatures enhance the folding kinetics for OmpA (22) and FomA (14). It was therefore anticipated that increasing the incubation temperature would promote the folding of all OMPs. However, observing the folding of nine OMPs in tandem revealed that the effect of temperature on folding efficiency was variable (Fig. 5).

One possible explanation for observed decrease in folding efficiency of some OMPs at higher temperatures may be aggregation. The first kinetic study of OmpA revealed that it can form an aggregated state that is off the pathway of the folding reaction (21). Because the folding kinetics of OmpA are also temperature-dependent (22), increases in temperature may promote this aggregated state in some OMPs. We are currently exploring this possibility.

Kinetic Experiments Reveal Novel Folding Phases—Our studies have recapitulated many of the observed trends in folding efficiencies that were established previously for OmpA. It has been shown that OmpA folding efficiency is promoted by thinner bilayers (20), higher pH values (12), smaller vesicles (20, 21), and higher temperatures (22). In this study, we tested the general applicability of the OmpA findings to a wide variety of *E. coli* proteins. We observed that OMPs demonstrate varied folding behaviors and sought to reconcile these differences by exploring the stability and kinetic behavior of each OMP.

The kinetic behaviors of the majority of these model OMPs are unknown. A thorough kinetic analysis has been published previously only for OmpA (14, 19–23). Although one study carried out under similar conditions reported a pseudo-first order rate constant on the same order of magnitude as the slow rates we have reported here, neither a fast rate nor a lag phase was observed (20). We postulate that the discrepancy between this and previous studies could simply be due to how the data were collected. The fast rates reported here ($10-80 \times 10^{-3}$ s^{-1}) have lifetimes of less than 120 s. Similarly, the lag phases are finished within 300 s. These phases could not be observed in any SDS-PAGE kinetic study to date because the earliest reported time point taken is at 60 s. Furthermore, the maximum number of time points observed in these experiments is 11 (12, 15, 20–22). From these 11 points, observed over several hours, various models have been fit even from the same set of data (14, 20).

To improve the density of the data over the rates we have reported, we collected a greater number of time points (13 points) over a shorter span of time (30 min). Furthermore, we repeated our experiments three times to show that the rates we reported were reproducible. Collecting data at these time points has shown the formation of OMP tertiary structure is subject to a fast rate and a lag phase.

We observed the lag phase and fast rate by only one technique, SDS-PAGE. Other techniques, such as circular dichroism (CD) and tryptophan fluorescence emission, can continuously observe the folding from the start of the reaction, and these spectroscopic techniques report on different aspects of the folding process. Tryptophan fluorescence emission changes as tryptophans move from a polar to an apolar environment, and CD tracks the formation of secondary structure. Where these techniques have been employed, they show no lag phase (12, 14, 15, 19–23). Kleinschmidt and Tamm (20) reported that CD and SDS-PAGE kinetics demonstrate similar kinetic rates and thus hypothesized that secondary and tertiary structure form at the same time. Because they used similar conditions as we did here and observed the folding by SDS-PAGE, only at later time points, it is possible that a lag phase of OmpA was

undetected in those experiments. This would mean that formation of secondary and tertiary structure is not as synchronized as proposed previously. Or, because we have shown that tertiary structure formation can be delayed by thicker bilayers, our data may suggest that these processes can be separated. These conjectures must be tested, but the presence of a lag phase in tertiary structure formation does indicate that the *in vitro* OMP folding pathway is more complex than previously considered.

OMPs Employ Various Folding Strategies—Previous kinetic studies have also hypothesized that OMPs of larger barrels have slower folding rates. This was based on a study of two proteins, OmpA and FomA, of different sizes from different organisms (14). The data shown here indicate that folding rates are not dictated solely by barrel size. In fact, we found that barrels of the same size can also demonstrate varied folding behavior. Of the eight-stranded barrels, OmpA and OmpX fold well under almost all conditions, whereas the folding efficiency of OmpW and PagP is much lower in equivalent conditions (Fig. 4). The ability for OmpX to fold so efficiently may be because it folds fastest (Fig. 8). However, the highly efficient folder OmpA has kinetic rate constants within one standard deviation of the rate constants that describe the eight-stranded OMPs that fold poorly, OmpW and PagP (Fig. 9). We postulate that OmpA may fold more efficiently in the lipid screen than OmpW and PagP for reasons due to other aspects of their kinetic behavior. OmpW demonstrates no burst phase, and PagP demonstrates the longest lag phase (Fig. 9), both of which may contribute to reduced levels of overall folding. OmpA is also more resistant to thermal denaturation than OmpW and PagP (Fig. 10) and is thus more likely to accumulate a larger folded population. Although OmpX, OmpW, OmpA, and PagP all have eight-stranded β-barrel motifs, they vary drastically in folding efficiency, kinetic profile, and resistance to thermal stability; thus we conclude that barrel size is not a sufficient rationalization to explain variations in folding behavior.

Barrels of various sizes, namely OmpX (8 strands), OmpA (8 strands), OmpT (10 strands), and Omp85 (12–16 strands), were able to fold into vesicles made from native lipid extracts (Fig. 3), whereas OmpW (8 strands), PagP (8 strands), OmpLa (12 strands), FadL (14 strands), and OmpF (16 strands) could not. Data from our folding studies in PC lipids can identify the strategies that permit some OMPs but not others to fold into native lipids. OmpA demonstrates the most resistance to thermal denaturation (Fig. 10), and perhaps it is this stability that provides the means for OmpA to fold into native lipids. However, such an argument is not adequate for all of the OMPs that can fold into native lipids. For example, Omp85 is the least resistant to thermal denaturation (Fig. 10) but also folds into native lipids (Fig. 3). The ability for Omp85, OmpT, and OmpX to fold into native lipids may be due to kinetic behavior. In $diC_{11}PC$, OmpX folding is completely dominated by the fast phase, and OmpT and Omp85 have equivalent contributions to the folding by the slow and fast phases. These kinetic profiles contrast with that of other OMPs, which are dominated by the slow phase. The faster folding phases of OmpX, OmpT, and Omp85 are more robust in thicker bilayers and may explain their ability to fold into native lipids.

Most interestingly, the kinetic and thermal denaturation analyses reveal that the most efficient folders employ different folding strategies. OmpX and OmpA demonstrate the highest folding efficiency under more conditions than any of the other OMPs, yet their folding behaviors vary. OmpA is the most resistant to thermal denaturation of the OMPs studied here, whereas OmpX is only moderately resistant to denaturation by temperature (Fig. 10). OmpX is the fastest folding protein, but OmpA folds only at moderate speeds (Fig. 8). It is likely that OmpX folding is driven by its kinetics, whereas OmpA achieves high folding efficiency because of its inherent stability.

Challenges in Measuring the Thermodynamic Stability of OMPs—We have shown that resistance to thermal denaturation varies between OMPs (Fig. 10), and this value may correlate to their folding efficiency (Fig. 4). However, our matrix revealed no conditions for which the thermodynamic equilibrium stability of all OMPs can be measured. In fact, such conditions have been reported only for OmpA (24–27). Tamm and colleagues have shown that OmpA is more stable in thicker bilayers (25), at neutral pH (26), and in the presence of PE lipids (26). Here we have shown that OmpA folding efficiency remains robust and almost invariable when we changed the same parameters (Figs. 4, 6, and 7). Although there seems to be disparity among these results, it must be recognized that the folding efficiency we have reported and the stability that Tamm and colleagues report (25, 26) are different metrics. Stability is an equilibrium measurement of the free energy of the folded state with respect to an unfolded state. In contrast, folding efficiency is the fraction of folded protein observed at a given time point and is influenced by both the stability and the kinetics of folding.

This comparison highlights an important challenge in studying the thermodynamic behavior of OMPs. We have shown that OmpA can completely fold on an experimentally accessible time scale, and these conditions must be met to measure the stability of any protein (54). Moreover, we show here that most other OMPs do not fold as efficiently as OmpA in almost all environments. This is problematic because the stability of a protein is influenced by its environment. If the stability of OMPs cannot be measured in the same environment, then their stabilities cannot be compared directly. Although considerable effort has produced conditions in which the stability of OmpA can be measured (24–27), more such effort will be necessary to find conditions in which the stability of all OMPs can be assessed.

Conclusion—The broad scan of folding conditions that we performed here serves as the starting point to explore the complexities of the folding behavior of all OMPs. Such investigations will explain the molecular basis of why proteins that have evolved to reside in the same biological membrane vary in their ability to fold. Understanding which protein characteristics promote folding will have a far reaching impact in structural biology, protein design, and medicine.

Acknowledgments—We gratefully acknowledge Michael McCaffery, of the Johns Hopkins University Integrated Imaging Center, for providing technical support for electron microscopy; Greg Bowman, for sharing the BL21(DE3) Star™ cells; and members of the Fleming group for helpful discussion.

REFERENCES

1. White, S. H. (2004) *Protein Sci.* **13,** 1948–1949
2. Kleffel, B., Garavito, R. M., Baumeister, W., and Rosenbusch, J. P. (1985) *EMBO J.* **4,** 1589–1592
3. Engelman, D. M., and Steitz, T. A. (1981) *Cell* **23,** 411–422
4. Schleiff, E., Eichacker, L. A., Eckart, K., Becker, T., Mirus, O., Stahl, T., and Soll, J. (2003) *Protein Sci* **12,** 748–759
5. Hill, K., Model, K., Ryan, M. T., Dietmeier, K., Martin, F., Wagner, R., and Pfanner, N. (1998) *Nature* **395,** 516–521
6. Casadio, R., Jacoboni, I., Messina, A., and De Pinto, V. (2002) *FEBS Lett.* **520,** 1–7
7. Lomize, M. A., Lomize, A. L., Pogozheva, I. D., and Mosberg, H. I. (2006) *Bioinformatics* (*Oxf.*) **22,** 623–625
8. Hessa, T., White, S. H., and von Heijne, G. (2005) *Science* **307,** 1427
9. Meindl-Beinker, N. M., Lundin, C., Nilsson, I., White, S. H., and von Heijne, G. (2006) *EMBO Rep.* **7,** 1111–1116
10. Bos, M. P., Robert, V., and Tommassen, J. (2007) *Annu. Rev. Microbiol.* **61,** 191–214
11. Surrey, T., and Jahnig, F. (1992) *Proc. Natl. Acad. Sci. U. S. A.* **89,** 7457–7461
12. Surrey, T., Schmid, A., and Jahnig, F. (1996) *Biochemistry* **35,** 2283–2288
13. Shanmugavadivu, B., Apell, H. J., Meins, T., Zeth, K., and Kleinschmidt, J. H. (2007) *J. Mol. Biol.* **368,** 66–78
14. Pocanschi, C. L., Apell, H. J., Puntervoll, P., Hogh, B., Jensen, H. B., Welte, W., and Kleinschmidt, J. H. (2006) *J. Mol. Biol.* **355,** 548–561
15. Huysmans, G. H., Radford, S. E., Brockwell, D. J., and Baldwin, S. A. (2007) *J. Mol. Biol.* **373,** 529–540
16. Osborn, M. J., Gander, J. E., Parisi, E., and Carson, J. (1972) *J. Biol. Chem.* **247,** 3962–3972
17. Kamio, Y., and Nikaido, H. (1976) *Biochemistry* **15,** 2561–2570
18. Seydel, U., Schroder, G., and Brandenburg, K. (1989) *J. Membr. Biol.* **109,** 95–103
19. Kleinschmidt, J. H., and Tamm, L. K. (1999) *Biochemistry* **38,** 4996–5005
20. Kleinschmidt, J. H., and Tamm, L. K. (2002) *J. Mol. Biol.* **324,** 319–330
21. Surrey, T., and Jahnig, F. (1995) *J. Biol. Chem.* **270,** 28199–28203
22. Kleinschmidt, J. H., and Tamm, L. K. (1996) *Biochemistry* **35,** 12993–13000
23. Kleinschmidt, J. H., den Blaauwen, T., Driessen, A. J., and Tamm, L. K. (1999) *Biochemistry* **38,** 5006–5016
24. Hong, H., Szabo, G., and Tamm, L. K. (2006) *Nat. Chem. Biol.* **2,** 627–635
25. Hong, H., and Tamm, L. K. (2004) *Proc. Natl. Acad. Sci. U. S. A.* **101,** 4065–4070
26. Tamm, L. K., Hong, H., and Liang, B. (2004) *Biochim. Biophys. Acta* **1666,** 250–263
27. Hong, H., Park, S., Jimenez, R. H., Rinehart, D., and Tamm, L. K. (2007) *J. Am. Chem. Soc.* **129,** 8320–8327
28. Mahalakshmi, R., Franzin, C. M., Choi, J., and Marassi, F. M. (2007) *Biochim. Biophys. Acta* **1768,** 3216–3224
29. Blattner, F. R., Plunkett, G., 3rd, Bloch, C. A., Perna, N. T., Burland, V., Riley, M., Collado-Vides, J., Glasner, J. D., Rode, C. K., Mayhew, G. F., Gregor, J., Davis, N. W., Kirkpatrick, H. A., Goeden, M. A., Rose, D. J., Mau, B., and Shao, Y. (1997) *Science* **277,** 1453–1474
30. Dekker, N., Merck, K., Tommassen, J., and Verheij, H. M. (1995) *Eur. J. Biochem.* **232,** 214–219
31. Sambrook, J., Fritsch, E. F., and Maniatis, T. (1989) *Molecular Cloning: A Laboratory Manual,* 2nd Ed., p. B.25, Cold Spring Harbor Laboratory Press, Cold Spring Harbor, NY
32. Inouye, M., and Yee, M. L. (1973) *J. Bacteriol.* **113,** 304–312
33. Nakamura, K., and Mizushima, S. (1976) *J. Biochem.* **80,** 1411–1422
34. Arora, A., Rinehart, D., Szabo, G., and Tamm, L. K. (2000) *J. Biol. Chem.* **275,** 1594–1600
35. Pautsch, A., Vogt, J., Model, K., Siebold, C., and Schulz, G. E. (1999) *Proteins* **34,** 167–172
36. Robert, V., Volokhina, E. B., Senf, F., Bos, M. P., Van Gelder, P., and Tommassen, J. (2006) *PLoS Biol.* **4,** e377
37. Stegmeier, J. F., and Andersen, C. (2006) *J. Biochem.* **140,** 275–283
38. Kramer, R. A., Zandwijken, D., Egmond, M. R., and Dekker, N. (2000) *Eur. J. Biochem.* **267,** 885–893
39. Pilsl, H., Smajs, D., and Braun, V. (1999) *J. Bacteriol.* **181,** 3578–3581
40. Black, P. N., Said, B., Ghosn, C. R., Beach, J. V., and Nunn, W. D. (1987) *J. Biol. Chem.* **262,** 1412–1419
41. Khalid, S., Bond, P. J., Carpenter, T., and Sansom, M. S. (2007) *Biochim. Biophys. Acta* 10.101b/j.bbamem.2007.05.024
42. Hong, H., Patel, D. R., Tamm, L. K., and van den Berg, B. (2006) *J. Biol. Chem.* **281,** 7568–7577
43. Basle, A., Iyer, R., and Delcour, A. H. (2004) *Biochim. Biophys. Acta* **1664,** 100–107
44. Bolter, B., Soll, J., Schulz, A., Hinnah, S., and Wagner, R. (1998) *Proc. Natl. Acad. Sci. U. S. A.* **95,** 15831–15836
45. Reumann, S., Davila-Aponte, J., and Keegstra, K. (1999) *Proc. Natl. Acad. Sci. U. S. A.* **96,** 784–789
46. Gentle, I., Gabriel, K., Beech, P., Waller, R., and Lithgow, T. (2004) *J. Cell Biol.* **164,** 19–24
47. Wilks, J. C., and Slonczewski, J. L. (2007) *J. Bacteriol.* **189,** 5601–5607
48. Moncelli, M. R., Becucci, L., and Guidelli, R. (1994) *Biophys. J.* **66,** 1969–1980
49. Laue, T. M., Shah, B., Ridgeway, T. M., and Pelletier, S. L. (1992) in *Analytical Ultracentrifugation in Biochemistry and Polymer Science* (Harding, S. E., Rowe, A. J., and Horton, J.C., eds) pp. 90–125, Royal Society of Chemistry, Cambridge, UK
50. Colbeau, A., Nachbaur, J., and Vignais, P. M. (1971) *Biochim. Biophys. Acta* **249,** 462–492
51. Pocanschi, C. L., Patel, G. J., Marsh, D., and Kleinschmidt, J. H. (2006) *Biophys. J.* **91,** L75–77
52. Lomize, A. L., Pogozheva, I. D., Lomize, M. A., and Mosberg, H. I. (2006) *Protein Sci.* **15,** 1318–1333
53. Lewis, B. A., and Engelman, D. M. (1983) *J. Mol. Biol.* **166,** 211–217
54. Stanley, A. M., and Fleming, K. G. (2008) *Arch Biochem. Biophys.* **469,** 46–66